12th International Symposium on Turbulence and Shear Flow Phenomena (TSFP12)
Osaka, Japan (Online), July 19-22, 2022

EQUILIBRIUM AND NON-EQUILIBRIUM SCALING RELATIONS IN ATMOSPHERIC BOUNDARY LAYER.

Marta Wacławczyk
Institute of Geophysics, Faculty of Physics
University of Warsaw
Pasteura 5, 02-093 Warsaw
marta.waclawczyk@fuw.edu.pl

Jakub Nowak
Institute of Geophysics, Faculty of Physics
University of Warsaw
Pasteura 5, 02-093 Warsaw
marta.waclawczyk@fuw.edu.pl

Szymon P. Malinowski
Institute of Geophysics, Faculty of Physics
University of Warsaw
Pasteura 5, 02-093 Warsaw
marta.waclawczyk@fuw.edu.pl

ABSTRACT

In this work we aim to retrieve information about temporal changes of turbulence in the atmosphere and leading-order terms in the budget of kinetic energy based on wind velocity measurements within the Atmospheric Boundary Layer (ABL). We focus on in-situ experiment performed by a research aircraft which flies horizontally and records current state of turbulence along its track. We calculate turbulence intensity and study its dependence on the integral length scale. We also calculate two non-dimensional indicators, the dissipation factor and the integral-to-Taylor scale ratio and plot them as a function of the Taylor-based Reynolds number. This allows to divide flow regions into areas of equilibrium and non-equilibrium turbulence. In the equilibrium turbulence energy spectra have a self-similar form and certain relations between the length scale and turbulence intensity hold, which allow to identify the leading-order terms in the energy balance. These relations take a different form in non-equilibrium turbulence, which is a sign of rapidly-changing external conditions.

INTRODUCTION

Turbulence plays an important role in the atmospheric dynamics. It dissipates energy at small scales, but also contributes to the unpredictability of the weather (Wyngaard, 2011). In spite of many measurement campaigns our knowledge on atmospheric turbulence is still far from sufficient due to limited amount of data and measurement errors. Observations in the atmosphere can be divided into in situ and remote sensing. In situ measurements require that the instruments be located directly at the point of interest, e.g. by installing them on a mast at certain, fixed heights. Another example are airborne measurements performed by research aircrafts, at altitudes higher than the heights of masts. Analysis of such measurement data is a subject of the current study.

Apart from calculating basic turbulence statistics, like the turbulence intensity $\mathscr{U}$, turbulence kinetic energy dissipation rate (EDR) ε and the integral length scale $\mathscr{L}$ along the flight track, we attempt to retrieve information on the temporal changes of turbulence. For this, we separately consider two distinct states of turbulence, 'equilibrium' and 'non-equilibrium'. The 'equilibrium' turbulence can be defined as a state where the classical Taylor's dissipation law holds

$$\varepsilon = C_\varepsilon \frac{\mathscr{U}^3}{\mathscr{L}}, \quad C_\varepsilon = const, \tag{1}$$

This cornerstone relation is a basis of many turbulence models. It also follows from Eq. (1) that

$$\frac{\mathscr{L}}{\lambda} = \frac{C_\varepsilon}{15} R_\lambda, \tag{2}$$

where $\lambda = \sqrt{15\nu/\varepsilon}\mathscr{U}$ is the Taylor's length scale and $R_\lambda = \mathscr{U}\lambda/\nu$ is the Taylor-based Reynolds number. Even though $C_\varepsilon = const$ does not depend on the Reynolds number, Bos *et al.* (2007) argued that in the decaying turbulence its value is typically about twice larger than in the stationary case where turbulence production balances the dissipation. This difference follows from a finite time needed for the energy injected at large scales to reach the dissipative end of the energy cascade. Moreover, if the equilibrium Taylor's law (1) holds, the classification of turbulence states can be made by studying balance of leading-order terms in the transport equation for turbulence kinetic energy. As it is discussed in the following, the balance between shear production and dissipation implies $\mathscr{L} \sim \mathscr{U}$, under the assumption of the constant shear. In the decaying turbulence, on the other hand, $\mathscr{L} \sim 1/\mathscr{U}^a$, with $a > 0$, (Sinhuber *et al.*, 2015).

A number of recent research works (Vassilicos, 2015; Seoud & Vassilicos, 2007; Valente & Vassilicos, 2011; Bos & Rubinstein, 2018; Bos *et al.*, 2007) questioned the validity of the scaling (1) and (2) in the presence of rapid time changes of the system. A different 'unusual' dissipation scaling was found in the laboratory experiments of Seoud & Vassilicos (2007) and Valente & Vassilicos (2011). Those authors argued that C_ε is not constant, but depends on the inlet conditions and local Reynolds number. Bos & Rubinstein (2018) derived

these non-equilibrium scaling laws for C_ε and $\mathscr{L}/\lambda$ based on theoretical arguments. They found

$$\frac{C_\varepsilon}{C_{\varepsilon 0}} \approx \left(\frac{R_{\lambda 0}}{R_\lambda}\right)^{15/14} \tag{3}$$

and

$$\frac{\mathscr{L}}{\lambda} \approx \frac{C_{\varepsilon 0}}{15} R_{\lambda 0}^{15/14} \left(\frac{1}{R_\lambda}\right)^{1/14}, \tag{4}$$

where $C_{\varepsilon 0}$ and $R_{\lambda 0}$ are the 'equilibrium' values of the non-dimensional dissipation parameter and Reynolds number. If turbulence decays C_ε becomes larger than the equilibrium value $C_{\varepsilon 0}$. On the other hand, if turbulence production is locally larger than the dissipation $C_\varepsilon < C_{\varepsilon 0}$.

The non-equilibrium relations (3) and (4) are substantially different from their equilibrium counterparts (1) and (2). Hence, classification of turbulence into 'equilibrium' and 'non-equilibrium' can be made on this basis. The purpose of this work is to use this procedure to analyse data recorded by a research aircraft in marine stratocumulus-topped ABL. In this case the flow conditions in the investigated region are unknown *a priori* and only limited information, that is 1D intersections of the flow field, along the flight track are available. We focus on the data from the recent ACORES campaign designed for the observations of Aerosol, Cloud, Turbulence, and Radiation Properties at the Top of the Marine Boundary Layer over the Eastern North Atlantic Ocean (Siebert *et al.*, 2021; Nowak *et al.*, 2021). From this campaing, high-resolution (100 Hz) data recorded by the ACTOS platform are available. We calculate turbulence statistics and the non-dimensional indicators C_ε and $\mathscr{L}/\lambda$ and plot them as a function of R_λ to identify whether turbulence is in or out-of equilibrium. Moreover, by investigating values of C_ε it is possible to divide the flow area into regions where turbulence decays, develops or is in a stationary state. Additional criterion which we consider is the dependence of $\mathscr{L}$ on $\mathscr{U}$, which allows to identify leading-order terms in the turbulence energy budget. We believe our study can deliver new, important information on the dynamics of turbulence in the atmosphere.

EQUILIBRIUM TURBULENCE

In the 'equilibrium' turbulence the Taylor's law (1) and Eq. (2) are satisfied. The constant C_ε in Eq. (1) may, however, be different in stationary and decaying or developing turbulence. As argued by Bos *et al.* (2007), it follows from the fact that there is a finite time $\mathscr{T}$ needed for the energy injected at large scales to reach the dissipative end of the energy cascade.

To study turbulence in the ABL we will consider turbulence kinetic energy (TKE) budget for horizontally homogeneous shear flow

$$\frac{\partial k}{\partial t} = T + P - \varepsilon + B, \tag{5}$$

where $k = \overline{u_i' u_i'}/2$, in the isotropic turbulence $k = 3/2\mathscr{U}^2$,

$$T = -\frac{1}{2}\frac{\partial \overline{u_i' u_i' w'}}{\partial z} - \frac{1}{\rho}\frac{\partial \overline{p' w'}}{\partial z}$$

is the turbulent transport, p' denotes fluctuations of the pressure, $w' = u_3'$ is the fluctuating vertical component of velocity,

$$P = -\overline{w' u_i'}\frac{\partial \overline{u_i}}{\partial z}$$

is the production term, $\varepsilon = 2\overline{s_{ij} s_{ij}}$, where $s_{ij} = (\partial u_i'/\partial x_j + \partial u_j'/\partial x_i)/2$ is the EDR and

$$B = \overline{b' w'}$$

denotes the buoyancy flux.

Balances of leading order terms in TKE equation were investigated e.g. in Yano & Wacławczyk (2022) to identify characteristic scales of atmospheric boundary-layer systems. We will also consider here several simplified cases, assuming that there are only two leading order terms in Eq. (5) which results in the balances between

1. shear production and dissipation: $P \sim \varepsilon$
2. buoyancy flux and dissipation $B \sim \varepsilon$
3. turbulent transport and dissipation: $T \sim \varepsilon$
4. time derivative and dissipation (decaying turbulence, no forcing): $\partial k/\partial t \sim -\varepsilon$

In case 1), using gradient diffusion hypothesis

$$\overline{w' u'} = -\nu_t \frac{\partial \overline{u}}{\partial z} \sim \mathscr{L}\sqrt{k}\frac{\partial \overline{u}}{\partial z}$$

and assuming $\partial \overline{u}/\partial z = S \approx const$ we obtain

$$P \sim \mathscr{L}\sqrt{k} S^2.$$

Using the equilibrium Taylor's law (1), which predicts $\varepsilon \sim k^{3/2}/\mathscr{L}$, for the balance $P \sim \varepsilon$ we obtain

$$\mathscr{L}\sqrt{k} S^2 \sim \frac{k^{3/2}}{\mathscr{L}},$$

hence

$$\mathscr{L}^2 \sim k, \quad \text{or} \quad \mathscr{L} \sim \mathscr{U}. \tag{6}$$

In the case of buoyancy-produced turbulence 2) we will assume that

$$B = \overline{w' b'} \approx const$$

and again make use of the equilibrium Taylor's law (1). With this for the balance $B \sim \varepsilon$ we obtain

$$B \sim \frac{k^{3/2}}{\mathscr{L}}, \quad \text{hence} \quad \mathscr{L} \sim k^{3/2} \quad \text{or} \quad \mathscr{L} \sim \mathscr{U}^3. \tag{7}$$

In case 3) where dissipation and advection are the leading-order terms in the TKE budget, we will use the gradient diffusion hypothesis to express the transport term as

$$T = -\frac{1}{2}\frac{\partial \overline{u_i' u_i' w'}}{\partial z} \sim \nu_t \frac{\partial k}{\partial z} \sim \mathscr{L}\sqrt{k}\frac{\partial k}{\partial z} \sim \mathscr{L}\sqrt{k}\frac{k}{\mathscr{L}}.$$

For the dissipation we will use the Taylor's law:

$$\varepsilon \sim k^{3/2}/\mathscr{L}.$$

Now, the balance $T \sim \varepsilon$ results in the identity relationship

$$\mathscr{L}\sqrt{k}\,\frac{k}{\mathscr{L}} \sim \frac{k^{3/2}}{\mathscr{L}}, \tag{8}$$

hence, in this case no correlation between k (or $\mathscr{U}$) and $\mathscr{L}$ is obtained.

Finally, in case 4) (decaying turbulence) we expect k and ε to decrease and $\mathscr{L}$ to increase in time (Sinhuber *et al.*, 2015)

$$k \sim t^{-n}, \quad \varepsilon \sim nt^{-(n+1)}, \quad \mathscr{L} \sim t^{1-n/2},$$

where the coefficient n is related to the scaling of the energy spectrum in low wavenumbers range. We assume

$$k^a \mathscr{L} = const,$$

where a is a constant. Differentiating above formula with respect to time

$$ak^{a-1}\frac{dk}{dt}\mathscr{L} + k^a\frac{d\mathscr{L}}{dt} = 0, \quad \text{hence} \quad a\frac{1}{k}\frac{dk}{dt} = -\frac{1}{\mathscr{L}}\frac{d\mathscr{L}}{dt}$$

Because $dk/dt < 0$ and $d\mathscr{L}/dt > 0$, hence we must have $a > 0$ and

$$\mathscr{L} \sim 1/k^a \quad \text{or} \quad \mathscr{L} \sim 1/\mathscr{U}^{2a}, \quad a > 0. \tag{9}$$

NON-EQUILIBRIUM TURBULENCE

The statistics of 'non-equilibrium' turbulence follow the formulas (3) and (4). Also in this case $C_\varepsilon > C_{\varepsilon 0}$ indicates decay of TKE whereas $C_\varepsilon < C_{\varepsilon 0}$ would describe developing turbulence, with production exceeding the dissipation (Bos & Rubinstein, 2018). The non-equilibrium scaling is found in the case of rapid changes of the system (e.g. changes of forcing), such that the turbulence energy spectrum have not had enough time to relax to its self-similar state. The non-equilibrium relation (3) will modify the scalings (6) and (7). Instead of the Taylor's law, the dissipation will be proportional to

$$\varepsilon \sim \frac{1}{R_\lambda^{15/14}}\frac{k^{3/2}}{\mathscr{L}}, \tag{10}$$

hence the leading-order balance between the production and dissipation gives

$$R_\lambda^{15/14}\mathscr{L}^2 \sim k, \quad \text{or} \quad R_\lambda^{15/28}\mathscr{L} \sim \mathscr{U}. \tag{11}$$

Instead of (7), for the balance $B \sim \varepsilon$ we obtain

$$\mathscr{L}R_\lambda^{15/14} \sim k^{3/2} \quad \text{or} \quad \mathscr{L}R_\lambda^{15/14} \sim \mathscr{U}^3. \tag{12}$$

No conclusion can be drawn for the balance $T \sim \varepsilon$. Possibly, the gradient diffusion relationship for the triple correlation term should be appropriately modified in this case. We still expect that the turbulence transport term will lead to decorrelation of $\mathscr{L}$ and $\mathscr{U}$.

For zero forcing (case 4) we assume (9) still holds, i.e. turbulence length scale is inversely proportional to $\mathscr{U}$.

SENSITIVITY STUDY

We analysed data of vertical wind velocity component w in marine ABL recorded during the ACORES campaign. In order to calculate turbulence statistics the instantaneous velocity should first be decomposed into the mean and fluctuating parts. In practice, in the atmospheric turbulence, the presence of large-scale convective motions and changes of atmospheric conditions along the flight track makes the choice of the averaging window difficult. In order to detrend the recorded signal we used the averaging window $AW_D = 50$s, the same as in Nowak *et al.* (2021) where the same ACORES data were analysed. Next, another window AW_S was used to calculate turbulence statistics from the detrended signal. We found that $AW_S = 150$s which corresponds to the window length larger than $20\mathscr{L}$ results in acceptable estimates of C_ε, (with standard deviations below 0.1). This window was moved every 5s along the signal and each time turbulence statistics were estimated. Turbulence intensity was calculated as $\mathscr{U} = \sqrt{\overline{w'^2}}$. The integral length scale $\mathscr{L}$ was estimated by integrating the transverse two-point correlation coefficient till the first zero-crossing and dividing the result by a factor 0.57, which, under additional assumptions should be equal to the longitudinal length scale (Wacławczyk *et al.*, 2022). We also assume here that the flow is locally isotropic, which is not always the case in marine stratocumulus-topped ABL (Akinlabi *et al.*, 2019; Nowak *et al.*, 2021), especially close to the cloud top, where a stably stratified layer is present. However, for data investigated here (from lower altitudes) our estimates should approximate the integral turbulence length scale.

To find the energy dissipation rate ε we assume the following form of the transverse second-order structure function, in accordance with the Kolmogorov's theory

$$S_\perp = \overline{(w'(x+r) - w'(x))^2} = C_\perp \varepsilon^{2/3} r^{2/3}, \tag{13}$$

where $C_\perp \approx 2.86$. We estimate ε by fitting the calculated $S_\perp$ in the inertial range to formula (13). Having $\mathscr{U}$, ε and $\mathscr{L}$ we calculated C_ε as defined in Eq. (1) as well as $\mathscr{L}/\lambda$ and studied its dependence on R_λ.

RESULTS

Most of the data points considered here (coupled stratocumulus case) follow the equilibrium scaling (1) and (2) (Wacławczyk *et al.*, 2022). Exception is for the data recorded at the lowest horizontal flight LEG of altitude 300 m, see Fig. 1. In this figure two parallel lines of a constant $C_{\varepsilon 0} = 0.45$ and $C_\varepsilon = 0.81$ are plotted. The first one corresponds to the equilibrium case with the production equal, approximately dissipation. The second value corresponds to a free self-similar decay of turbulence with zero production. The mean value of C_ε in this region is equal, approximately $C_\varepsilon \approx 0.25$ and is lower than $C_{\varepsilon 0}$, which suggests strong turbulence production and developing turbulence. Non-equilibrium scaling is also found for $\mathscr{L}/\lambda$, see Fig. (2).

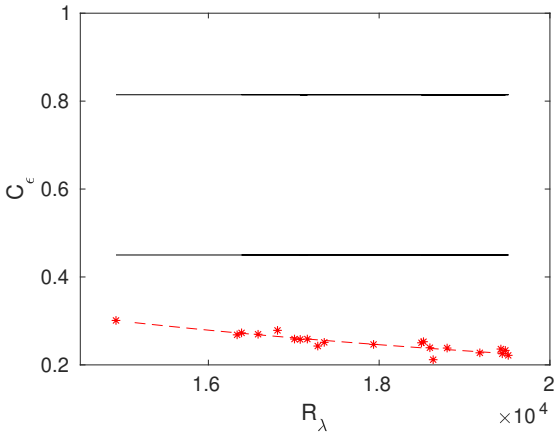

Figure 1. Marine ABL, data for horizontal flight LEG at altitude 300m. C_ε as a function of R_λ. Solid black lines - equilibrium scalings $C_{\varepsilon 0} = 0.45$ and $C_{\varepsilon 1} = 1.81 C_{\varepsilon 0}$, dashed red line - non-equilibrium scaling, Eq. (3), calculated statistics: symbols.

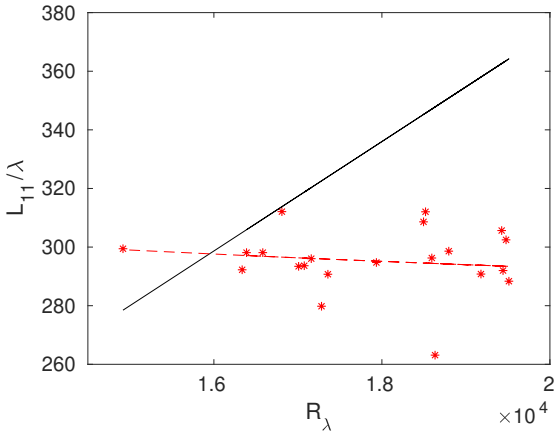

Figure 2. Marine ABL, data for horizontal flight LEG at altitude 300m. $\mathscr{L}/\lambda$ as a function of R_λ. Solid black line - equilibrium scaling (2), dashed red line - non-equilibrium scaling, Eq. (4), calculated statistics: symbols.

To additionally evaluate the data we studied the dependence of $\mathscr{L}$ on $\mathscr{U}$ and R_λ. The scaling seems to follow relation (11), where we assume $15/28 \approx 1/2$, see Fig. (3)

Data recorded during horizontal flight at altitude 550m follow the equilibrium scaling (1) and (2). In this region, below the cloud, turbulence production is much weaker and the mean value of $C_\varepsilon \approx 0.55$ is larger than the equilibrium value $C_{\varepsilon 0}$. The integral length scale $\mathscr{L}$ becomes inversely proportional to $\mathscr{U}$, which suggests that the scaling (9) holds, see Fig. 4. Here, scatter of the data is larger, which can indicate the role of turbulent transport which leads to decorrelation of $\mathscr{L}$ and $\mathscr{U}$.

The highest horizontal flight considered here was performed at altitude 800m, inside the stratocumulus cloud. Values of C_ε changed along the flight track considerably, suggesting that the region of weaker turbulence alternate with areas of strong turbulence production. In spite of these variations C_ε and $\mathscr{L}/\lambda$ follow, in selected areas, the equilibrium scaling relations (1) and (2) which can be interpreted as a form of quasi-equilibrium, i.e. the function passes through series of

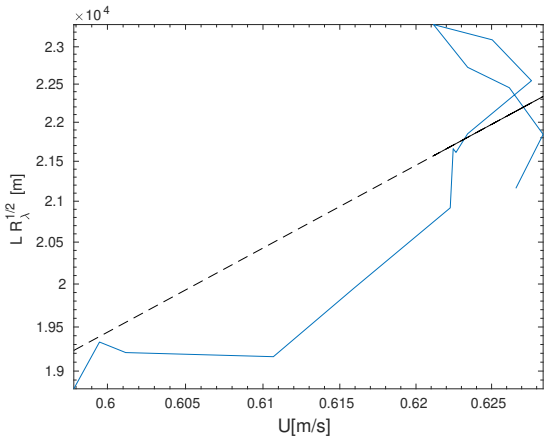

Figure 3. Marine ABL, data for horizontal flight LEG at altitude 300m. $\mathscr{L}\sqrt{R_\lambda}$ as a function of $\mathscr{U}$ follows the non-equilibrium scaling relation (11).

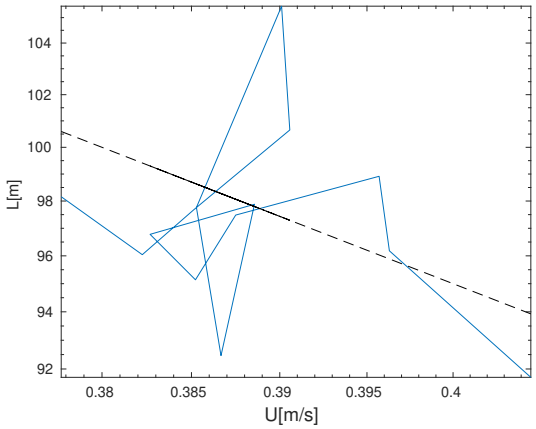

Figure 4. Marine ABL, data for horizontal flight LEG at altitude 550m. $\mathscr{L}$ as a function of $\mathscr{U}$ follows the scaling relation (9).

equilibrium states. Dependence of $\mathscr{L}$ on $\mathscr{U}$ clearly follow relation (7), which indicates dominant role of buoyancy and dissipation in the energy balance, see Fig. 5.

CONCLUSIONS

We presented estimates of non-dimensional indicators C_ε and $\mathscr{L}/\lambda$, as well as dependence of $\mathscr{L}$ on $\mathscr{U}$ from in-situ measurements inside marine ABL, performed by a research aircraft during ACORES campaign. We focused on the horizontal flight legs of the length of several kilometers. Stable conditions along the flight track allow to calculate statistics such as the turbulence length scale $\mathscr{L}$ with a sufficient accuracy. We found that at the lowest flight leg at the altitude of 300m $C_\varepsilon < C_{\varepsilon 0}$ which suggest that strong turbulence production takes place there. Statistics follow the non-equilibrium scaling relations. Weaker turbulence is found at higher altitude of 550m, below the cloud, where $C_\varepsilon > C_{\varepsilon 0}$ and $\mathscr{L}$ becomes inversely proportional to $\mathscr{U}$. Inside the cloud C_ε varies considerably, however dependence of $\mathscr{L}$ on $\mathscr{U}$ suggest the leading order balance between the buoyancy production and dissipation in TKE budget. The analyses performed here can be repeated for other measurement data in ABL's. This can im-

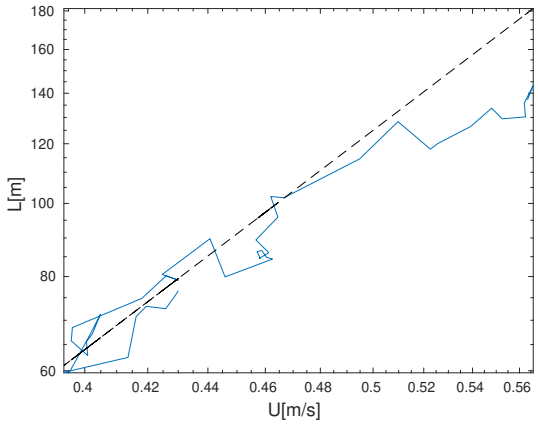

Figure 5. Marine ABL, data for horizontal flight LEG at altitude 800m. $\mathscr{L}$ as a function of $\mathscr{U}$ follows the scaling relation (7).

prove parametrizations of turbulence in the atmosphere, which is crucially important for numerical weather predictions and climate models.

ACKNOWLEDGEMENTS

The financial support of the National Science Centre, Poland (Project No. 2020/37/B/ST10/03695) is gratefully acknowledged.

REFERENCES

Akinlabi, Emmanuel O., Wacławczyk, Marta, Mellado, Juan Pedro & Malinowski, Szymon P. 2019 Estimating turbulence kinetic energy dissipation rates in the numerically simulated stratocumulus cloud-top mixing layer: Evaluation of different methods. *Journal of the Atmospheric Sciences* **76** (5), 1471 – 1488.

Bos, W.J.T. & Rubinstein, R 2018 Dissipation in unsteady turbulence. *Phys. Rev. Fluids* **2**, 022601(R).

Bos, W.J.T., Shao, L. & Bertoglio, J.-P. 2007 Spectral imbalance and the normalized dissipation rate of turbulence. *Phys. Fluids* **19**, 045101.

Nowak, J. L., Siebert, H., Szodry, K.-E. & Malinowski, S. P. 2021 Coupled and decoupled stratocumulus-topped boundary layers: turbulence properties. *Atmospheric Chemistry and Physics* **21** (14), 10965–10991.

Seoud, R. E. & Vassilicos, J. C. 2007 Dissipation and decay of fractal-generated turbulence. *Physics of Fluids* **19** (10), 105108.

Siebert, Holger, Szodry, Kai-Erik, Egerer, Ulrike & et al. 2021 Observations of aerosol, cloud, turbulence, and radiation properties at the top of the marine boundary layer over the eastern north atlantic ocean: The acores campaign. *Bulletin of the American Meteorological Society* **102** (1), E123 – E147.

Sinhuber, M., Bodenschatz, E. & Bewley, G. P. 2015 Decay of turbulence at high reynolds numbers. *Phys. Rev. Lett.* **114**, 034501.

Valente, P. C. & Vassilicos, J. C. 2011 The decay of turbulence generated by a class of multiscale grids. *Journal of Fluid Mechanics* **687**, 300–340.

Vassilicos, J. C. 2015 Dissipation in turbulent flows. *Annu. Rev. Fluid Mech.* **47**, 95–114.

Wacławczyk, M., Nowak, J. L., Siebert, H & Malinowski, S. P. 2022 Detecting non-equilibrium states in atmospheric turbulence. *submitted to J. Atmos. Sci.* .

Wyngaard, J. C. 2011 *Turbulence in the atmosphere*. Cambridge University Press.

Yano, J-I & Wacławczyk 2022 Nondimensionalization of the atmospheric boundary-layer system: Obukhov length and monin–obukhov similarity theory. *Boundary Layer Meteorology* **182**, 417–439.